

Birefringent common-path interferometer for testing large convex spherical surfaces

Yang Xiang

Caixin Xiang

Academia Sinica

Changchun Institute of Optics and Fine
Mechanics

State Key Laboratory of Applied Optics

P.O. Box 1024

Changchun 130022, China

Guodong Zhang

Northeast Normal University

Department of Physics

Changchun 130024, China

Abstract. A new birefringent common-path interferometer with an automatic data-processing system is presented for testing large convex spherical surfaces. With this interferometer, it is easier to eliminate system errors and to achieve quite accurate measurement. The precision of the system is about $\lambda/50$ with an accuracy of about $\lambda/10$.

Subject terms: birefringent common-path interferometers.

Optical Engineering 32(5), 1080–1083 (May 1993).

1 Introduction

The testing of large convex spherical surfaces is a troublesome problem that needs to be overcome. Testing using a Twyman or Fizeau interferometer with a reference surface is very expensive. Holographic phase conjugate interferometers have been developed,^{1,2} but they are rather difficult to fabricate and inconvenient. We have developed a birefringent common-path interferometer with an automatic data-processing system for the testing of large convex spherical surfaces. We hope it is helpful in practical use.

2 Configuration and Principle

Both the configuration and principle of the interferometer are shown in Fig. 1. This interferometer is composed of two principal parts. One is the interferometer objective, which is composed of a piece of a large lens and a small birefringent lens consisting of two glass lenses and one calcite lens placed between the two glass lenses. The apertures of the large lens and the small birefringent lens are ϕ 230 and 20 mm, respectively. The relative aperture of the interferometer objective is 1/9.1. The other is an automatic data sampling and processing system, which consists of a TV camera with 512×512 pixels, a 12-bit analog-to-digital (A/D) converter, and 640-Kb IBM microcomputer. The light source is a 2-mW linearly polarized He-Ne laser. The collimated laser beam from the beam expander and splitter is divided into an *O* (ordinary) and an *E* (extraordinary) beam by the birefringent lens. The *O* beam is focused at point *A* after passing through the large lens. The *E* beam is focused on a ϕ 5-mm film, coated on the rear surface of the large lens, and reflected back to the TV

camera. (The film used here is to reduce the transmissivity of the light to avoid the background fringes and increase the fringe contrast. If the large lens is thick enough or the radius curvature of its front surface is quite different from its thickness, this film may not be required.)

First, a small fine convex (or concave) spherical mirror with surface error $< \lambda/20 \sim \lambda/30$, an aperture of ϕ 30 mm, and a ratio of 1:5 for the aperture to radius of curvature, is placed so that its center of curvature coincides with point *A*. Retroreflected from the small fine spherical mirror, the *O* beam interferes with the *E* beam on the TV camera.

According to the fringe analysis method,³ the coordinates of the fringe peaks are extracted and numbered by the horizontal scanning of the vertical interference fringes. This process is repeated at intervals until the whole interferogram has been scanned. These data are put into the optical path difference (OPD) simultaneous equations consisting of the 37-term Zernike polynomials $Z_n^l(x,y)$. By solving these simultaneous equations by the least-squares method,⁴ we can obtain the OPD between the *O* and *E* wave fronts:

$$W_1(x,y) = \sum_{n=0}^k \sum_{l=-n}^n C_{nl} Z_n^l(x,y) \quad (1)$$

$$= W_r(x,y) - [W_n(x,y) + W_m(x,y)] \quad (2)$$

where C_{nl} is the aberration coefficient, $W_r(x,y)$ is the total wave-front aberration of the inverse reflected *E* light through the birefringent lens, $W_n(x,y)$ is the total wave-front aberration of the retroreflected *O* light through the birefringent lens and the large lens, and $W_m(x,y)$ is the surface error of the small fine spherical mirror. Because $W_m(x,y) \ll W_n(x,y)$, formula (2) may be reduced to

$$W_1(x,y) = W_r(x,y) - W_n(x,y) \quad (3)$$

Paper 13062 submitted by *Acta Optica Sinica*; received June 14, 1992; accepted for publication Oct. 24, 1992.

© 1993 Society of Photo-Optical Instrumentation Engineers. 0091-3286/93/\$2.00.

BIREFRINGENT COMMON-PATH INTERFEROMETER

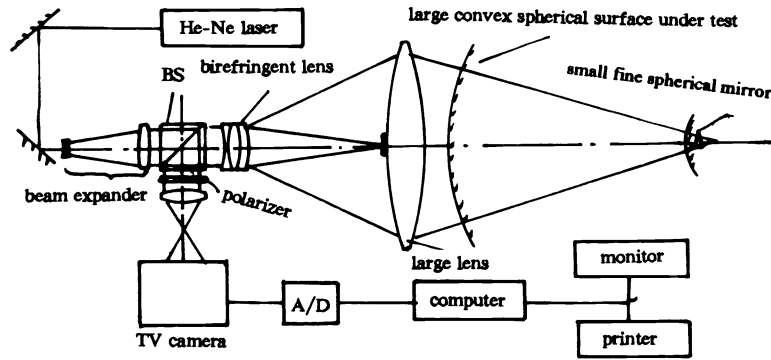


Fig. 1 Birefringent common-path interferometer used for testing large convex spherical surfaces.

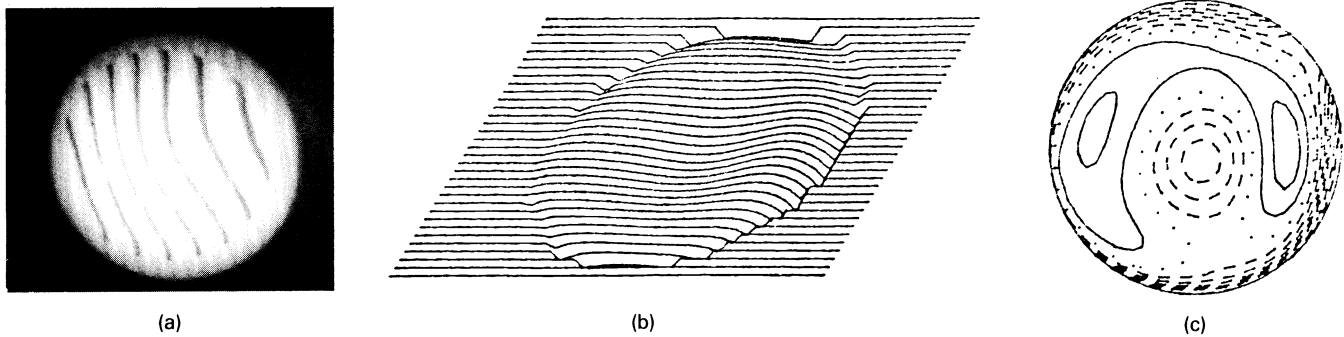


Fig. 2 (a) The interferogram, (b) 3-D plots, and (c) contour of $W_1(x,y)$, respectively; points sampled = 229, PV = 0.31 W, rms = 0.002 W, and contour step = 0.025 W.

To avoid the wave aberration change effect resulting from the deformation propagation of the wave front⁵ so that the OPD $W_1(x,y)$ maintains the form of formula (2), and to ensure that there are not more fringes in the interferometric field, $W_r(x,y)$ and $W_n(x,y)$ must be less than λ .

Then, the large convex spherical surface to be tested is placed in front of the interferometer objective and its center of curvature is coincident with point A. The OPD $W_2(x,y)$ between the O wave front retroreflected from the large convex spherical surface being tested and the E wave front inversely reflected from the rear surface of the large lens is:

$$W_2(x,y) = \sum_{n=0}^k \sum_{l=-n}^n C'_{nl} Z_n^l(x,y) \quad (4)$$

$$= W_r(x,y) - [W_n(x,y) + W_t(x,y)] \quad (5)$$

where $W_t(x,y)$ is the surface error of the large convex spherical surface and C'_{nl} is the wave aberration coefficient. From formulas (1), (3), (4), and (5), we obtain the surface error $W_t(x,y)$ of the large convex spherical surfaces being tested. {If $[W_r(x,y) - W_n(x,y)] = W_m(x,y)$, $W_t(x,y)$ may be evaluated by using formulas (1), (2), (4), and (5).}:

$$\begin{aligned} W_t(x,y) &= W_1(x,y) - W_2(x,y) \\ &= \sum_{n=0}^k \sum_{l=-n}^n (C_{nl} - C'_{nl}) \cdot Z_n^l(x,y) \quad (6) \end{aligned}$$

Now, the peak-to-valley value (PV) and rms of the large convex spherical surface can be obtained from formula (6).

3 Results and Accuracy of Measurement

According to the measuring principle presented above, $W_1(x,y)$ is tested first and stored in the computer, then $W_2(x,y)$ is tested. The surface error $W_t(x,y)$ of the large convex spherical surface being tested may be obtained by subtracting $W_2(x,y)$ from $W_1(x,y)$ and eliminating all the defocus effects.⁶ The test results of a large convex surface, with a 200-mm aperture and a ratio of 1:10 for the aperture to radius of curvature, are given in Figs. 2, 3, and 4.

The precision of the fringe analysis method is $PV < \lambda/50$ and $rms < \lambda/150$. Because the distortion effect of a TV camera is the same for $W_r(x,y)$ and $W_n(x,y)$, according to formulas (3) and (5), it does not affect the measured values of $W_1(x,y)$, $W_2(x,y)$, and $W_t(x,y)$. According to formulas (2) and (5), the accuracy of $W_t(x,y)$ is:

$$\Delta W_t(x,y) = \Delta W_1(x,y) + \Delta W_2(x,y) + \Delta W_m(x,y) < \lambda/10 \quad (7)$$

4 Conclusion

Provided that the interferometer objective is assembled compactly, $W_1(x,y)$ almost remains constant. Thus, during a certain test period, $W_t(x,y)$ of each sample can be obtained only by testing the $W_2(x,y)$ and subtracting it from $W_1(x,y)$, which was tested at the beginning of the test and stored as a correcting constant in the computer. Therefore, this method is very simple and easy to apply in practice.

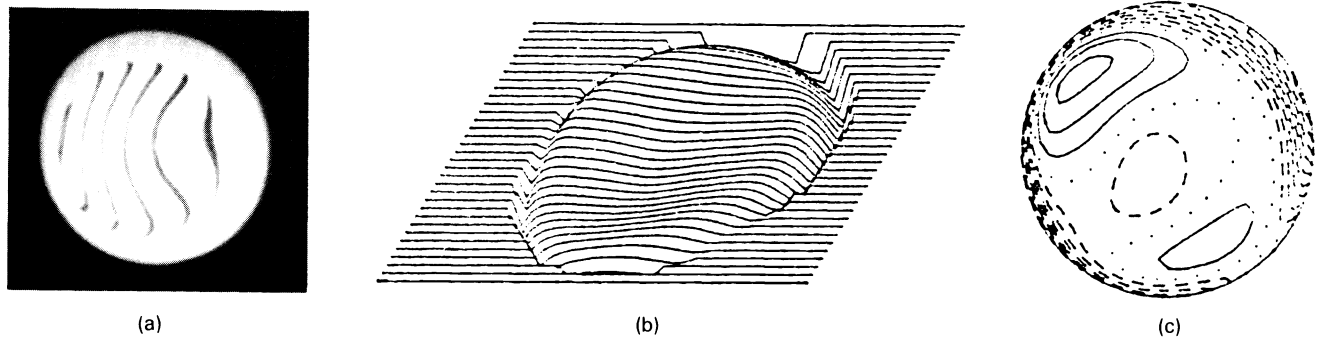


Fig. 3 (a) The interferogram, (b) 3-D plots, and (c) contour of $W_2(x,y)$, respectively; points sampled = 184, PV = 0.63 W, rms = 0.11 W, and contour step = 0.05 W.



Fig. 4 (a) The 3-D plots and (b) contour of the surface error $W_1(x,y)$ of the large convex spherical surface being tested; PV = 0.59 W, rms = 0.006 W, contour step = 0.05 W.

The large lens used does not need to be of very fine quality. The measurement accuracy is dependent only on the surface error of the small fine spherical mirror and is not affected by the distortion of the TV camera, therefore, we can obtain a more accurate measurement by using a small spherical mirror of fine quality, which demonstrates that this method can achieve higher measuring accuracy.

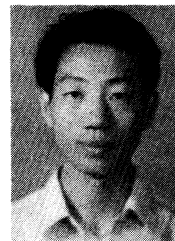
The birefringent common-path interferometer is easier to fabricate than the holographic phase-conjugate interferometer. It also has advantages over the holographic phase-conjugate interferometer in the areas of fringe contrast and operation.

In the method presented, the aperture and relative aperture of the interferometer objective should be larger than those of the large convex spherical surface to be tested. According to the above discussion, this interferometer can test a much larger convex spherical surface if the aperture and relative aperture of the interferometer objective are large enough. We still need to develop an interferometer objective with variable focal lengths for testing large convex spherical surfaces with various aperture-to-radius ratios.

References

1. A. B. Zenzinov and A. A. Schetnikov, "Application of the holographic wave-front correction method in interferometry to monitor the shape of a reflecting surface," *Opt. Spectrosc. (USSR)* **56**(4), 435-436 (1984).
2. Z. Zou, J. Liao, Y. Gu, and Q. Gu, "An interferometric method for measuring an optical spherical surface using holographic phase conjugate compensation," *Acta Opt. Sinica (China)* **6**(4), 360-364 (1986).
3. E. Bernal and J. S. Loomis, "Interactive video image digitizer—

- application to interferogram analysis," *Proc. SPIE* **126**, 143-151 (1977).
4. J. S. Loomis, *FRINGE User's Manual*, Optical Sciences Center, University of Arizona (1976).
 5. C. Xiang, "Deformation propagation of wavefront," *Opt. Fine Mechan. (China)* **3**, 1-7 (1979); C. Xiang and Y. Xiang, "The system error of the collimating lens in unequal-path Twyman interferometer," *Opt. Fine Mechan. (China)* **1**, 22-24 (1989).
 6. K. Yasuda, K. Satoh, and M. Suzuki, "Fringe analyzer for a Fizeau interferometer," *Proc. SPIE* **1163**, 181-187 (1989).



Yang Xiang received his BS degree in physics in 1985 and MS degree in theoretical physics in 1988, both from Northeast Normal University, China. Since 1988, he has worked at the State Key Laboratory of Applied Optics, Changchun Institute of Optics and Fine Mechanics, Academia Sinica, China, where he now is a research associate. His research interests include surface testing, signal and image processing, and interferometric testing.



Caixin Xiang is a professor of optics and image-quality evaluation. He graduated from the Department of Physics, Wuhan University, China, in 1955. Since then he has worked on optical testing and image quality evaluation at Changchun Institute of Optics and Fine Mechanics, Academia Sinica, China. His research interests include star testing, optical transfer function testing, image quality evaluation, surface quality inspection, optical materials testing, length measurement, interferometric testing, and theory of image formation, coherence, and interferometers. Xiang has published more than 40 papers in his research areas.



Guodong Zhang received the BS degree in physics from Jilin University, Changchun, in 1965. From 1973 to 1988, he worked in optical design and optical information processing at Changchun Institute of Optics and Fine Mechanics, Academia Sinica, China. Since 1988, he has been performing research work in optical holography and coherent optical data processing at Northeast Normal University, Changchun, China. Zhang has published a number of papers on his research areas.